Evaluation of geosynthetic performance for permeable pavement subbase layer

Sharif Hossain & Jeongho Oh
Korea National University of Transportation, Korea

Shin In Han
Seo Yeong Engineering Co. Ltd., Korea

ABSTRACT: An extensive effort is actively being made to implement permeable pavement systems in urban or residential areas of South Korea in order to achieve an efficient water circulation system based on a low impact development (LID) design concept. This paper describes the work to evaluate the performance of geosynthetic-reinforced crushed stone subbase for permeable pavement systems, based on experimental programs. In addition, a discrete element based numerical analysis was conducted to characterize the relationship between crushed stone particle distribution and geosynthetic aperture size. From this assessment, the geosynthetic-reinforced crushed stone subbase for permeable pavement systems seems to be promising to provide better load bearing capacity in case of water infiltration throughout the substructure layer. In addition, a discrete element modeling was successfully employed to find that the average particle size (D50) needs to be around 60 percent of the inscribed circle's diameter of geosynthetic aperture.

Keywords: permeable pavement system; geosynthetic; crushed stone subbase; discrete element modeling; and load bearing capacity

1 INTRODUCTION

The primary function of the permeable pavement is to store stormwater until it infiltrates through the subgrade soil, and to carry low volume traffic load adequately during service lives. Generally, permeable pavements are categorized as porous asphalt (PA), pervious concrete (PC), and permeable interlocking concrete pavers (PICP) (Kayhanian *et al*., 2105). Similar to most urban areas in other countries, the majority of urban areas in South Korea have been paved specifically so that stormwater can be drained through drainage facilities. However, the mode of rainfall during summer season in South Korea has been gradually changing, so it is not uncommon to have high intensity rainfall within short time duration. This situation leads to frequent flooding that yields a significant amount of damage for urban infrastructure, and unsafe conditions for public lives. Therefore, extensive efforts are being made to implement a permeable pavement system to mitigate repetitive hazards. The Seoul metropolitan government reported that the portion of permeable pavements in Seoul was only three percent in 2014. They plan to increase the portion of the permeable pavement system by 60 percent by 2020 (Seoul Metropolitan Government, 2013). The benefits of permeable pavements include noise reduction, stormwater runoff volume management, and impact on urban heat island. With respect to noise reduction, when tires are rolling over permeable friction course, air in the tire treads is able to escape through the air void or pores of the mixture. Therefore, the noise generated by the tire and pavement can be reduced (Arambula *et al*., 2013). It has also been reported that the development of urban heat islands is attributed to solar reflectance of paving materials (Rose *et al*., 2003; Millstein, 2013). Although the application of full-depth permeable pavements are generally installed in urban parking lots and commercial and residential driveways, it is anticipated that such pavements can also be subjected to low/ medium traffic loads due to the high density of population in Seoul. In this case, the role of pavement sublayers becomes increasingly detrimental in case of surface runoff infiltration. The material within the pavement substructure experiences repetitive load and environmental effects, such as moisture content variation and extensive temperature change, which typically leads to the decrease of

load bearing capacity. Consequently, the geosynthetics have widely been utilized to: improve the load bearing capacity of soil or backfill deposits, prevent segregation of materials, and facilitate drainage condition. Recently, several studies have been conducted to reinforce ballast material, which is a sort of crushed stone material using geogrid. A permanent deformation test of geogrid-reinforced ballast specimens was conducted using a large-scale triaxial test device, along with numerical simulation based on discrete element method (DEM) (Qian *et al*., 2013). In accordance with the reference (Tayabji, 2015; Weiss *et al*., 2015), the use of geomembrane (impermeable liner) is recommended for permeable interlocking concrete pavement (PICP) to restrict infiltration into the expansive fill soils close to buildings. In this study, the use of the geosynthetic material for the permeable pavement system was investigated based on both experimental and numerical approaches, since the permeable pavement system in South Korea seems to subject a low-to- medium traffic level, if necessary.

2 FIELD EXPERIMENTAL PROGRAM

The researchers conducted field tests to evaluate the performance of a geosynthetic-reinforced crushed stone subbase layer for the permeable pavement system. For the purpose of this, a series of standard plate load, repetitive plate load, and light weight deflectometer (LWDT) tests were performed on the test section.

2.1 *Field test program*

The Stormwater Center at the University of New Hampshire provided recommendation on aggregate gradations for choker, filter, and reservoir courses (UNHSC, 2009). In this study, the gradation of choker course (AASHTO No. 57) was regarded as reference accounting for domestic aggregate commercial market situations. The maximum aggregate size was 25 mm, and the coefficient of uniformity (Cu) and gradation (Cc) was 1.6 and 0.9, respectively. In addition to the gradation, the maximum abrasion loss for 500 revolutions is obtained as 20.6%, satisfying the criteria of 50% (UNHSC, 2009). The subgrade soil was classified as SW soil, having 5% of plastic limit, and 4% of fine materials passing No. 200 sieve. With respect to the geosynthetic material, a unique type of geosynthetic was designed and manufactured as shown in Figure. 1. The geosynthetic material was made of polypropylene, with a series of punched structures. One cell has nine square elements (80*80 mm) composed of four isosceles triangles each. Each square element is connected by a circular cone-shape junction to enhance the load transfer efficiency. The tensile strength was 200 kN/m at 5 % strain/min rate from the laboratory test result conducted in accordance with ASTM D 6637 (ASTM, 2001).

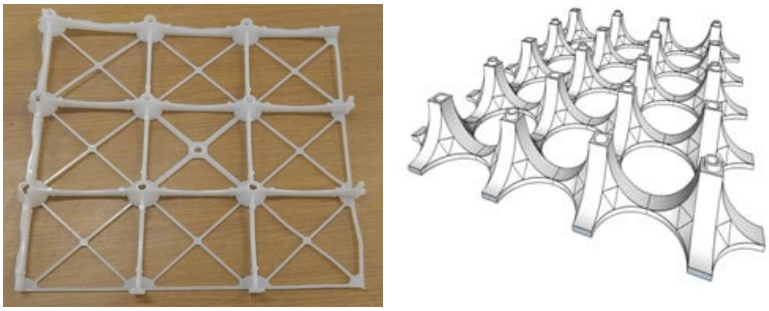

Figure 1. Geosynthetic material used**.**

The field test section is composed of three square segments as illustrated in Figure. 2. Each test segment is 4.0 m long and wide. The geosynthetic material was installed in different locations of the crushed-stone subbase layer based on review of previous research studies (Al-Qadi *et al*., 2008; Abu-Farsakh and Chen, 2011). Figure. 3 illustrates the construction procedure and field test programs. The first test section was excavated by 1 m and the roller compaction was utilized to compact natural subgrade soil by the thickness of 0.5 m. After the completion of subgrade compaction, crushed stone subbase layer was compacted every 10 cm. For the geosynthetic installation, 3.0 m long and wide, better interlocking was found to be achieved in case of placing the geosynthetic material on top of a loose aggregate layer (10 cm thick in compacted state), sandwiching it by another layer of loose aggregate (10 cm thick in compacted state) and then compacting both layers together to the target compaction state. A similar procedure to install geogrid was also found to be effective (Abu-Farsakh and Chen, 2011). For each segment, a series of field

tests was carried out to evaluate the performance of geosynthetic- reinforced crushed stone subbase, including light weight deflectometer testing (LWDT) to check the uniformity of compaction in accordance with ASTM E2835-11, and the standard and repeated plate load tests to examine the load bearing capacity of crushed stone subbase.

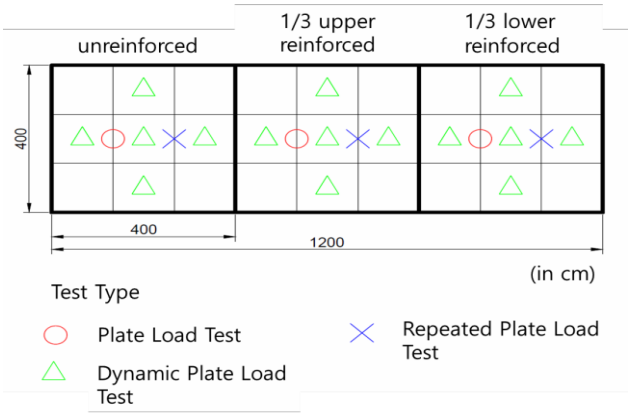

Figure 2. Scheme of field test section.

Figure 3. Procedure of field tests.

2.2 *Field test results*

LWDT tests were conducted during construction procedure to check the uniformity of compaction of the crushed stone subbase layer in accordance with (ASTM, 2011). It is reported that the compaction level for the choker, filter, and reservoir courses need to be 95% (UNHSC, 2009). However, there is no guideline on how to check the level of compaction. Since these materials are different with typical flexible base materials in terms of gradation, it is difficult to check the level of compaction using the nuclear density gage or sand cone method. In accordance with DIN 18 196, there is a guideline on how to check the compaction level along with the elastic dynamic modulus (E_{vd}) obtained from LWDT for different classified materials (Deutsches Institut für Normung e.V, 2011). The elastic dynamic modulus can be determined as follows.

$$E_{vd} = 1.5r\frac{\Delta\sigma}{\Delta z} \quad (1)$$

where E_{vd} is the deformation modulus of the subsoil, r is the radius of the plate (150 mm), $\Delta\sigma$ is the change in mean contact pressure, and Δz is the corresponding vertical displacement of the plate.
For the 97 % compacted gravel materials, the elastic dynamic modulus needs to be at least 35 MPa according to its guideline. In this study, the level of target compaction was set to be 95 %, and five measurements made for every segment were then averaged for this purpose. By interpolating the correlation between elastic dynamic modulus and compaction level given in the reference (Deutsches Institut für Normung e.V, 2011), the dynamic modulus equivalent to 95% compaction was found to be 27.5 MPa. All the segments exhibited an average value close to 30 MPa, which is slightly over the target value. This indicates that all test segments were generally compacted uniformly. The standard plate load test was then conducted in accordance with KSF 2310 (Korean Standards and Certifications Institute, 2015). Fig. 4 shows the load-settlement curves obtained from the test. The results revealed that geosynthetic-reinforced segments seem to perform better than unreinforced segments. In addition, as the magnitude of load increases, the difference between the two curves of reinforced segments also increases, yielding less ultimate settlement from the segment reinforced at upper 1/3 of crushed stone layer. Using Eq. (2), the subgrade reaction of modulus k30 was computed.

$$k_{30} = \frac{\sigma}{\delta} \quad (2)$$

Where σ is a corresponding normal stress in kPa when the vertical settlement is equal to 1.25 mm, and δ = vertical settlement equal to 1.25 mm. Table 1 summarizes the computed k_{30} values along with reinforcement effectiveness.

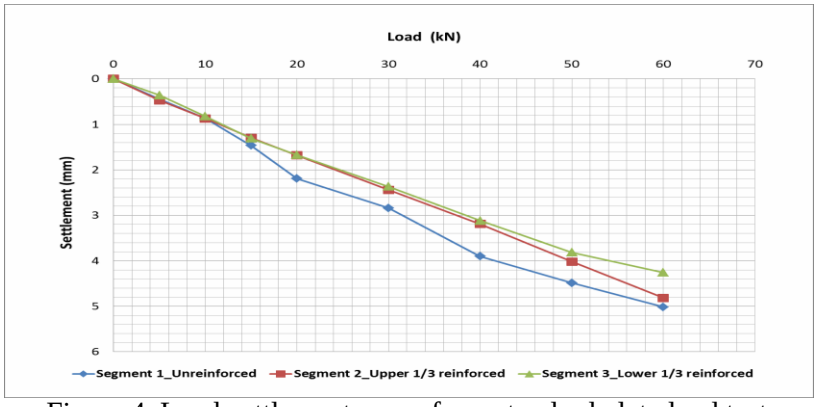

Figure 4. Load-settlement curve from standard plate load tests.

Table 1. Summary of plate load test results.

Segment Condition	k_{30}(kgf/ cm^3)	Effectiveness (%)
Unreinforced	14.3	-
Upper 1/3 reinforced	17.8	24.6
Lower 1/3 reinforced	18.4	28.6

As shown in Table 1, the subgrade reaction modulus values of reinforced segments were higher than that of the unreinforced segment, which results in 25~30 % of reinforcement effectiveness. In accordance with Korea roadway design specification (Infrastructure and Transport, 2013), the subgrade reaction modulus at 1.25 mm settlement needs to be greater than 20 kgf/cm^3 for subbase layer. The obtained values did not meet the requirement but the value from geosynthetic-reinforced segments seems to be compatible since it is expected that the permeable pavement system may have less traffic-induced stresses within the subbase layer. This also indicates the necessity of geosynthetic reinforcement for the permeable pavement system to support low-to- middle level of traffic load.

3 PARAMETRIC NUMERICAL ANALYSIS

The numerical modeling was performed using the Particle Flow Code (PFC), which is based on the DEM using spherical particles with deformable contacts and breakable bonds in between (Itasca, 2003). The objective of parametric numerical analysis is to quantify the optimum grain size distribution of crushed stone materials that yield the most effective interlocking with geosynthetic application.

3.1 *Modeling of crushed stone subbase*

The grain size distribution of crushed stone materials varied with respect to the AASHTO #57 aggregate size distribution for the parametric numerical analysis as shown in Figure. 5. The average particle size (D_{50}), which is representing the aggregate diameter corresponding to the 50 percent of passing, was regarded as reference to differ the distribution of grains. Stahl and Konietzky (2011) found that three constant values for shear stiffness, normal stiffness, and friction coefficient are sufficient to simulate the mechanical response in terms of stress and deformation under various loading conditions. In this study, the clump model available in PFC 3D was employed to represent angularity of grains. Clumps model arbitrarily shaped rigid bodies. The pebbles comprising a clump can overlap but contacts do not exist between them; instead, contacts form between the pebbles on the boundary of a clump and other bodies (Sikemeier, 2016). For simplicity, it is assumed the normal and shear stiffness are identical for the subbase materials. The normal and shear stiffness was assigned as 8.0E+4 (N/m) for the crushed stone materials regardless of the distribution of grain based on try-and-error yielding a reasonable deformation with a given loading condition.

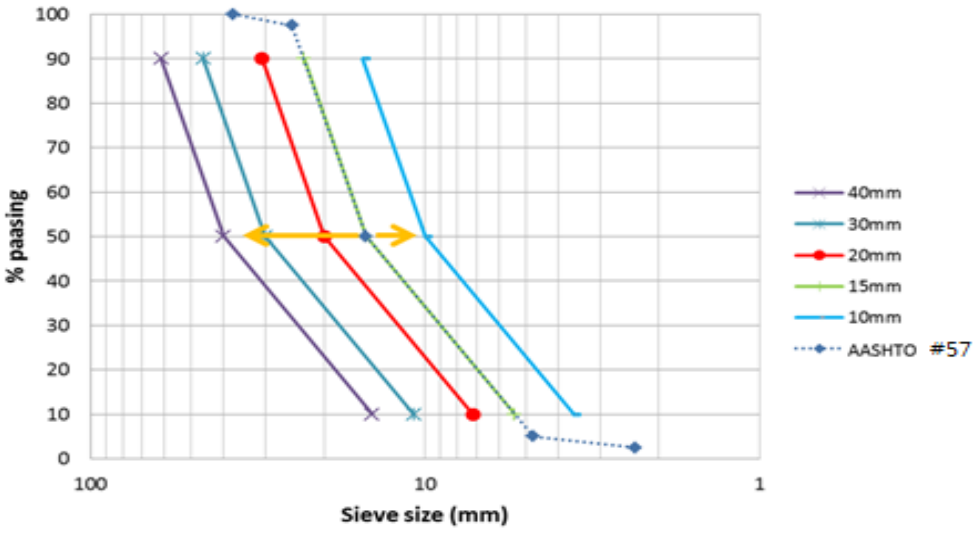

Figure 5. Variation of grain size distribution for parametric numerical analysis.

3.2 *Modeling of geosynthetic material*

The geosynthetic material was modeled by series of overlapping spherical particles of varying size, which accurately describe the geometrical aspects. A parallel bond was used to bond the individual particles together at each contact point, and this model was also successfully applied in a previosu study (Stahl and Konietzky, 2011). The calibration was first performed in terms of tensile strength to model the geosynthetic material used. A two-directional tension test was simulated in order to obtain the force of 2.4 kN at 5% strain that results in tensile stiffness of 200 kN/m based on the geometric condition of geosynthetic material as shown in Figure. 6. The calibrated normal and shear stiffness of the geosynthetic material was found to be 7.6E+7 (N/m) from this analysis. The ratio of the stiffness of aggregate to geosynthetic seems to be reasonable based on previous research studies (Konietzky *et al*., 2004; Chen *et al*., 2012).

3.3 *Modeling of repeated compression test*

The repeated compression test was simulated to investigate the degree of interlocking between the geosynthetic material and the particles, which is deemed similar loading condition obtained in the repeated plate load test. Each set of particles, having different distributions, was randomly scattered into the box and 30 kPa of distributed load was then applied to achieve dense condition as illustrated in Figure. 7. After that, repeated compression force in the y direction was applied on the geosynthetic by 0.01 mm/step rate. The numerical analysis indicated that as the average particle size increased from 10 to 20 mm, greater contact stress was obtained from interface between the particles and geosynthetic material. The contact stress shown in Figure. 8. tends to decrease beyond 20 mm of average particle size due to the increase of larger aggregate portion compared to grid size (33.14 mm diameter of inscribed circle as illustrated in Figure. 6), leading to the alleviation of interlocking behavior. In spite of limited numerical verification, it was observed that the optimum average particle size needs to be around 60 percent of the inscribed circle's diameter of geosynthetic aperture.

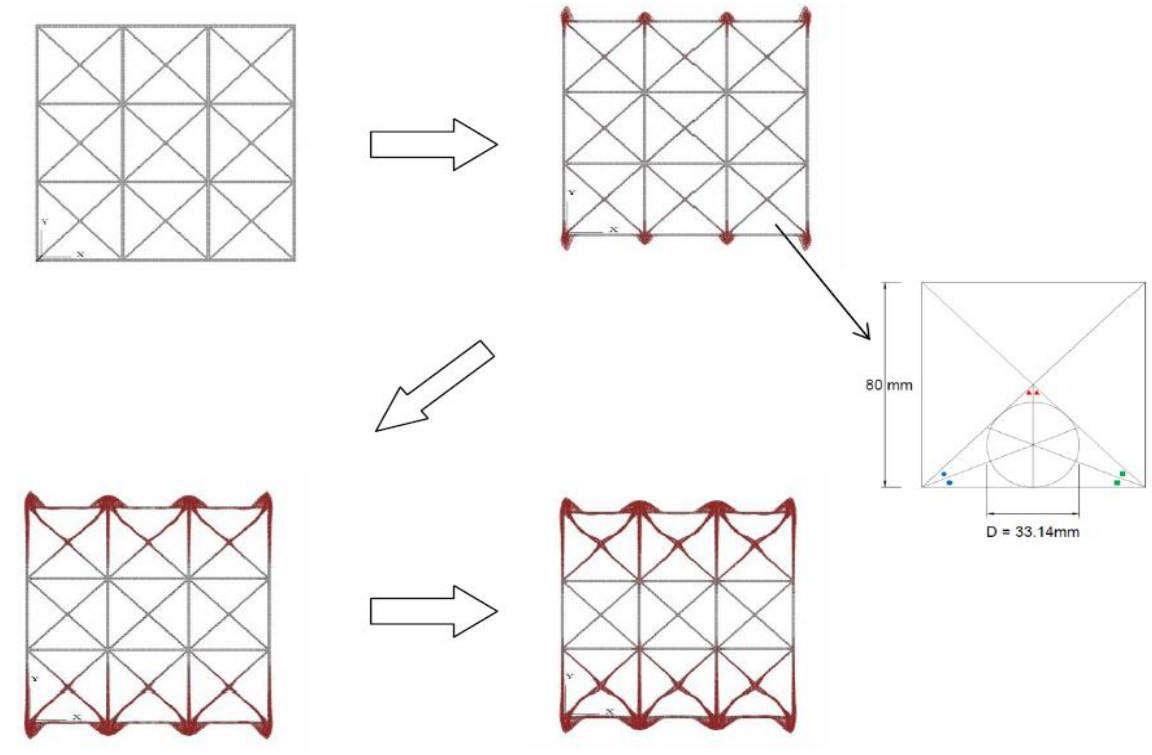

Figure 6. Modeling of tension test for the geosynthetic material.

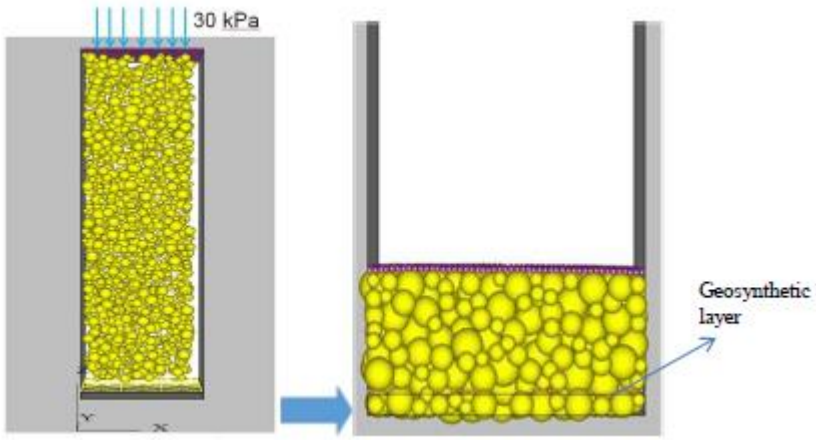

Figure 7. Simulation process of repeated compression test.

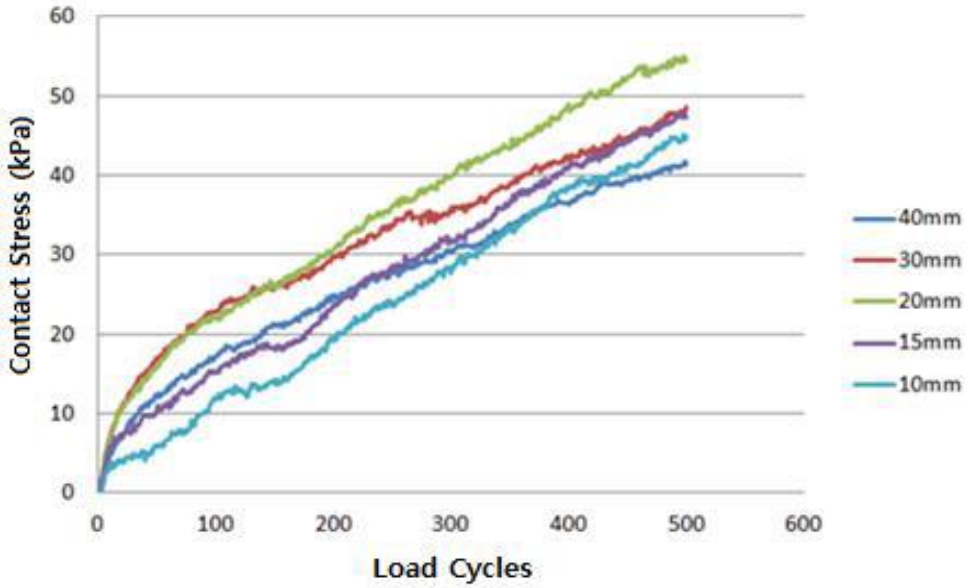

Figure 8. Results of numerical analysis.

4 CONCLUDING REMARKS

The necessity of permeable pavement systems becomes increasingly crucial in urban areas in order to maintain the sustainability of infrastructure and quality of residence lives. In this study, experimental and numerical programs were conducted to evaluate the geosynthetic- reinforced crushed stone subbase as the substructure of permeable pavement systems, in order to support low-to-medium levels of traffic. The following conclusions were drawn:

- The control of crushed stone subbase compaction is significantly important to ensure permeable pavement serviceability. It is considered LWDT is a useful tool in the assessment of the uniformity of compaction. In this study, 27.5 MPa of E_{vd} was set to be target value to achieve 95% compaction level for crushed stone subbase layer. Further investigations need to correlate in-situ density and LWDT measurements.
- Standard and repeated plate load tests exhibited that the load bearing capacity of geosynthetic-reinforced crushed stone subbase was improved by 10~30 percent when the geosynthetic was installed at lower on-third position of subbase.
- The deformation modulus of E_{v2} obtained from repeated plate load test is considered to be meaningful rather than E_{v1} since the value appears to represent elasto-plastic behavior of material and capture the interlocking behavior between geosynthetic material and surrounding aggregates.
- The numerical analysis revealed that the optimum average particle size needs to be around 60 percent of the inscribed circle's diameter of geosynthetic aperture. In other words, if the crushed stone materials have a gradation similar to AASHTO #57 for permeable pavement systems, the aperture size of the geosynthetic material used in this study needs to be slightly reduced, and this needs to be verified in further field evaluations.

ACKNOWLEDGMENT

This work was sponsored in part through the Korea Agency for Infrastructure Technology Advancement. The authors acknowledge the cooperation of the LID research center of Busan National University.

REFERENCES

Al-Qadi, I. L., Dessouky , S.H., Kwon, J., and Tutumluer, E. (2008). "Geogrid in flexible pavements" *Journal of the Transportation Research Board*, No. 2045, pp. 102–109, DOI: 10.3141/2045-12.

Arambula, E., Estakhri, C.K., Martin, A.E., Trevino, M., Smit, A., and Prozzi, J. (2013). "Performance and cost effectiveness of permeable friction course (PFC) pavements." Research Report, FHWA/TX-12/0-5836-2, Texas A&M Transportation Institute, College Station, TX, 2013.

ASTM International. (2001). ASTM D 6637. Standard Test Method for Determining Tensile Properties of Geogrids by the Single or Multi-Rib Tensile Method, Annual Book of ASTM Standards, West Conshohocekn, P.A.

ASTM International. (2011). ASTM E2835-11. Standard Test Method for Measuring Deflections Using a Portable Impulse Plate Load Test Device Annual Book of ASTM Standards. Vol. 04.03, West Conshohocken, PA.

Chen, C., McDowell, G.R., and Thom, N.H. (2012). "Discrete element modeling of cyclic loads of ge ogrid-reinforced ballast under confined and unconfined conditions" *Geotextiles and Geomembranes* 35, pp 76-86., DOI: 10.1016/j.geotexmem.2012.07.004.

Deutsches Institut für Normung e.V. (2011). DIN 18 196. "Earthworks and foundations; soil classification for civil engineering purposes." Berlin. Beuth Verlag GmbH, 10772 Berlin, Germany.

Infrastructure and Transport. (2013) Guideline for Roadway Construction and Design in Practice, Minis try of Land.

Itasca Consulting Group, Inc. (2003). PFC3D-Particle Flow Code in 3 Dimensions. Ver. 3.0 User's Man ual, Minneapolis, Minnesota, USA.

Kayhanian, M., Weiss, P.T., Gulliver, J.S., and Khazanovich, L. (2015). "The application of permeable pavement with emphasis on successful design, water quality benefits, and identification of knowledge and data gaps." A National Center for Sustainable Transportation Summary Report.

Konietzky, H., Kamp, L., and Groeger, T. (2004). "Use of DEM to model the interlocking effect of ge ogrids under static and cyclic loading" *Numerical Modeling in Micromechanics via Particle Methods. Shimizu, Hart & Cundall* (eds.), pp. 3-11, DOI: 10.1201/b17007-3.

Korea Rail Network Authority. (2011). Guideline for Railroad Design in Practice.

Korean Standards and Certifications Institute (2015). KS F 2310 Standard Test Method for Plate Load Test on Soils for Road.

Millstein, D. (2013). "Cool communities: Benefits of Cool Pavements in CA Cities". *Presented at the 2013 International Concrete Sustainability Conference. San Francisco, CA* .

Qian, Y., Mishra, D., Tutumluer, E., and Kwon, J. (2013). "Comparative evaluation of different aperture geogrids for ballast reinforcement through triaxial testing and discrete element modeling" 2013 Geosynthetics Conference, Long Beach, CA, Apr.

Rose, L., Akbari, H., and Taha, H. (2003). "Characterizing the Fabric of the Urban Environment": A Case Study of Metropolitan Houston. TX. LBNL-51448. (Accessed July 8, 2016). Lawrence Berkeley National Laboratory, Berkeley, CA."

Seoul Metropolitan Government. (2013). Master Plan to Maintain Effective Water Circulation System in Urban Area.

Siekmeier, J. (2016). "Geogrid reinforced aggregate base stiffness for mechanistic pavement design" Re search Project Final Report 2016-24. Minnesota Department of Transportation, MN, US.

Stahl, M., Konietzky, H (2011). "Discrete element simulation of ballast and gravel under special consid eration of grain shape, grain-size and relative density" Granular Matter, Vol. 13, Springer, Berlin, pp. 417-428., DOI: 10.1007/s10035-010-0239-y.

UNHSC (University of New Hampshire Stormwater Center). (2009). UNHSC design specifications for porous asphalt pavement and infiltration beds. University of New Hampshire, Durham, NH .

Weiss, P.T., Kayhanian, M., Khazanovich, L., and Gulliver, J.S. (2015). "Permeable pavements in cold climates: State of the Art and Cold Climate Case Studies." Research Report MN/RC 2015-30, University of Minnesota, MN.